Phase Behavior and Thermal Properties for Binary Blends of Compositionally Fractionated Poly(3-hydroxybutyrate-*co*-3-hydroxypropionate)s with Different Comonomer Composition

Yang-Ho Na, Yousuke Arai, Naoki Asakawa, Naoko Yoshie, and Yoshio Inoue*

Department of Biomolecular Engineering, Tokyo Institute of Technology, 4259 Nagatsuta-cho, Midori-ku, Yokohama, Kanagawa 226-8501, Japan

Received February 13, 2001; Revised Manuscript Received April 20, 2001

ABSTRACT: Bacterially synthesized poly(3-hydroxybutyrate-*co*-3-hydroxypropionate) [P(3HB-*co*-3HP)] samples were compositionally fractionated using solvent/nonsolvent fractionation techniques. Binary blends between these compositionally fractionated P(3HB-*co*-3HP) samples, with much narrower comonomer compositional distribution, were prepared, and their thermal and crystallization behavior were studied using differential scanning calorimeter (DSC) and polarized optical microscopy. It was found that, in the amorphous phase of these blends, the miscibility mainly depends on the difference of 3HP contents (or 3HB contents) between the two components of the blend. When the difference of 3HP content between two copolyesters is less than 30−40 mol %, they become miscible in the amorphous phase. The type of crystal lattice, miscibility, and difference of the spherulite growth rate between the two components of the blend appear to be the important factors controlling the crystalline phase behavior. The results are compared with those of unfractionated P(3HB-*co*-3HP)s and the effects of comonomer composition and its distribution on the properties of unfractionated copolymers are discussed.

Introduction

Poly(3-hydrobutyrate) [P(3HB)] and its copolymers with hydroxyalkanoates are thermoplastic polyesters, occurring as body inclusions in a large variety of microorganisms in nature. These polyesters are found to have potential uses in many application fields.[1−3] They include the copolyesters with 3-hydroxyvalerate (3HV),[4−6] 3-hydroxypropionate (3HP),[7−11] and 4-hydroxybutyrate (4HB).[12−14] It has been reported that these bacterially produced copolyesters have some broad comonomer compositional distribution.[14−21] Experimentally, poly(3-hydroxybutyrate-*co*-3-hydroxyvalerate)s [P(3HB-*co*-3HV)],[18,20,21] poly(3-hydroxybutyrate-*co*-3-hydroxypropionate)s [P(3HB-*co*-3HP)],[15,22] and poly(3-hydroxybutyrate-*co*-4-hydroxybutyrate)s [P(3HB-*co*-4HB)][14] were fractionated using solvent/nonsolvent techniques.[14,18,20−24] It has been demonstrated that broad comonomer compositional distributions were present in bacterially harvested copolyester products. Thus, the physical properties of bacterially synthesized copolyesters are not simply related to their comonomer contents, even for random copolyesters. To elucidate the correlation between the average comonomer content and the physical characteristics of bacterial copolyesters, an investigation of both average composition and compositional distribution are needed for strict physical characterization of the bacterial copolyesters.

Some studies on the relationship between physical properties and compositional distribution have been reported on the blends of P(3HB) and P(3HB-*co*-3HV) and the blends of P(3HB-*co*-3HV)s.[25−28] The binary blends are miscible when the relative 3HV content (i.e., difference between the average 3HV content of the two blend component copolyesters and the 3HV content of the component copolyesters) is smaller than about 12%, but immiscible when the difference exceeds it.[28] Miscibility and the crystallization rate may be important factors that affect the crystalline phase behavior. The results of thermal investigation have been compared with those of bacterially as-produced P(3HB-*co*-3HV) copolymers. According to the crystalline structure, P(3HB-*co*-3HV) copolyesters show the isodimorphic phenomenon, i.e., the 3HV units are included in the P(3HB) crystalline lattice and vice versa,[2] but P(3HB-*co*-3HP)s do not show such phenomenon.[22,29,30] Generally other hydroxyalkanoate copolymers seem to be more similar to P(3HB-*co*-3HP) than P(3HB-*co*-3HV) in the point of isodimorphism. In the experiments on P(3HB-*co*-3HP) blends, the type of crystal lattice should be considered in order to understand the relationships between various properties and compositional distribution. In this paper, the thermal and crystallization properties of P(3HB-*co*-3HP) blends are investigated by using binary blends of P(3HB-*co*-3HP)s with narrow comonomer compositional distribution, selected on the basis of the crystal lattice types. We study the effects of broad comonomer compositional distribution on the physical properties of unfractionated P(3HB-*co*-3HP)s with broad compositional distribution which should be considered as the blends of P(3HB-*co*-3HP)s with different 3HP contents. To the best of our knowledge, no studies have been carried out on bacterial copolymers which have no ability to cocrystallize except of course for P(3HB-*co*-3HV) blends.

Experimental Section

Materials. Bacterial homopolyester P(3HB), purchased from Aldrich Chem. Inc. (Lot No. 00925KF), was used after purification with chloroform and *n* -hexane. P(3HP), chemically synthesized through a ring-opening polymerization of propiolactone, was supplied by Tokuyama Co. (Tsukuba, Japan), which was also purified in the same way as P(3HB). Three

* To whom correspondence should be addressed. E-mail: yinoue@bio.titech.ac.jp.

10.1021/ma010270h CCC: $20.00 © 2001 American Chemical Society
Published on Web 06/09/2001

Table 1. Characteristics of the Fractionated P(3HB-*co*-3HP)s, P(3HB), and P(3HP)[a]

sample code	$M_n \times 10^{-5}$	M_w/M_n	crystal lattice type	original sample (before fractionation)
P(3HB)	2.13	1.52	P(3HB)	–
P(3HB-*co*-11.3%3HP)	2.97	1.99	P(3HB)	P(3HB-*co*-19.4%3HP)
P(3HB-*co*-14.9%3HP)	4.64	2.04	P(3HB)	P(3HB-*co*-19.4%3HP)
P(3HB-*co*-15.9%3HP)	2.57	2.34	P(3HB)	P(3HB-*co*-36.5%3HP)
P(3HB-*co*-23.8%3HP)	2.40	2.51	P(3HB)	P(3HB-*co*-36.5%3HP)
P(3HB-*co*-39.0%3HP)	4.99	2.36	amorphous	P(3HB-*co*-19.4%3HP)
P(3HB-*co*-48.0%3HP)	1.65	3.43	amorphous	P(3HB-*co*-36.5%3HP)
P(3HB-*co*-53.1%3HP)	3.09	1.90	amorphous	P(3HB-*co*-36.5%3HP)
P(3HB-*co*-60.1%3HP)	3.33	2.12	amorphous	P(3HB-*co*-36.5%3HP)
P(3HB-*co*-68.7%3HP)	2.14	2.95	P(3HP)	P(3HB-*co*-68.1%3HP)
P(3HB-*co*-77.9%3HP)	1.87	3.08	P(3HP)	P(3HB-*co*-68.1%3HP)
P(3HB-*co*-86.2%3HP)	2.45	1.45	P(3HP)	P(3HB-*co*-68.1%3HP)
P(3HB-*co*-89.6%3HP)	1.83	2.22	P(3HP)	P(3HB-*co*-68.1%3HP)
P(3HB-*co*-95.5%3HP)	2.50	1.76	P(3HP)	P(3HB-*co*-68.1%3HP)
P(3HP)	1.54	2.32	P(3HP)	–

[a] Notes: M_n and M_w/M_n are experimental data which were obtained using GPC of polystyrene standards. These are influenced by the finite composition distribution of the individual fractions, for the hydrodynamic volumes of chains are changed by a specimen's compositional distribution.

Table 2. Blending Type and Difference in 3HP Content between Component Polyesters of Blends

sample code	blend type	difference in 3HP content%
P(3HB)/P(3HB-*co*-11.3%3HP)	3HB-rich/3HB-rich	11.3
P(3HB)/P(3HB-*co*-14.9%3HP)	3HB-rich/3HB-rich	14.9
P(3HB)/P(3HB-*co*-23.8%3HP)	3HB-rich/3HB-rich	23.8
P(3HB-*co*-15.9%3HP)/P(3HB-*co*-23.8%3HP)	3HB-rich/3HB-rich	7.9
P(3HP)/P(3HB-*co*-68.7%3HP)	3HP-rich/3HP-rich	31.3
P(3HP)/P(3HB-*co*-86.2%3HP)	3HP-rich/3HP-rich	14.8
P(3HB-*co*-68.7%3HP)/P(3HB-*co*-95.9%3HP)	3HP-rich/3HP-rich	27.2
P(3HB)/P(3HB-*co*-77.9%3HP)	3HB-rich/3HP-rich	77.9
P(3HB-*co*-15.9%3HP)/P(3HB-*co*-77.9%3HP)	3HB-rich/3HP-rich	62.0
P(3HP)/P(3HB-*co*-11.3%3HP)	3HP-rich/3HB-rich	88.7
P(3HB)/P(3HB-*co*-39.0%3HP)	3HB-rich/amorphous	39.0
P(3HB-*co*-14.9%3HP)/P(3HB-*co*-53.1%3HP)	3HB-rich/amorphous	38.2
P(3HB-*co*-48.0%3HP)/P(3HB-*co*-60.1%3HP)	amorphous/amorphous	12.1
P(3HP)/P(3HB-*co*-48.0%3HP)	3HP-rich/amorphous	52.0
P(3HP)/P(3HB-*co*-60.1%3HP)	3HP-rich/amorphous	39.9
P(3HB-*co*-60.1%3HP)/P(3HB-*co*-68.7%3HP)	amorphous/3HP-rich	8.6
P(3HB-*co*-60.1%3HP)/P(3HB-*co*-89.6%3HP)	amorphous/3HP-rich	29.5

kinds of P(3HB-*co*-3HP) samples with 3HP contents of 19.4, 36.5, and 68.1 mol % were biosynthesized by the bacteria *Alcaligenus latus* (ATCC 29713) fed on the mixed carbon substrates of sucrose, (*R*)-3-hydroxybutyric acid [(*R*)-3HBA] and 3-hydroxypropionic acid [3HPA]. Fractionation of as-produced P(3HB-*co*-3HP) sample was carried out in chloroform/*n*-heptane mixed solvents, with *n*-heptane being carefully added to the solution under gentle agitation at 0−2 °C. This procedure was repeated until the addition of a large amount of *n*-heptane hardly caused any appreciable precipitation. The procedures of biosynthesis and fractionation are already described in detail in our previous work.[22,31] The results of the fractionation are tabulated in Table 1.

A previous report, based on the wide-angle X-ray diffraction (WAXD) of P(3HB-*co*-3HP)s, showed that 3HB-rich (0−38.3 mol % 3HP) and 3HP-rich (77.9−100 mol % 3HP) copolyesters form distinct helix structures, while copolyesters with 3HP monomer fractions ranging from about 45 to 75 mol % appear as the amorphous state.[22] The structural results were confirmed by the analysis of solid-state ^{13}C NMR and enzymatic biodegradation experiments.[29,30] The crystal pattern of P(3HB-*co*-3HP)s was determined by WAXD results in our previous article.[22] To examine exactly the effect of compositional distribution on the phase behavior and properties, several simple binary blends were prepared from the compositionally fractionated bacterial P(3HB-*co*-3HP) with much narrower comonomer compositional distribution, which were selected by the types of crystal lattices. These blend samples were binary blends of (a) two polyester samples both of which form P(3HB)-lattice type crystals [HB + HB], (b) two polyester samples both of which form P(3HP)-lattice type crystals [HP + HP], (c) the first one and the other one, which form the P(3HB)- and the P(3HP)-lattice type crystals, respectively [HB + HP], and (d) the combinations of the P(3HB)- or P(3HP)- type crystalline polyester and amorphous polyester [HB or HP + AM]. The film samples of P(3HB-*co*-3HP), P(3HB), P(3HP), and the binary blends with weight ratios of 75/25, 50/50 and 25/75 were prepared by solvent casting. After casting, the solvent (chloroform) was allowed to evaporate at room-temperature overnight, and then the blends were dried for 3 days under vacuum. Furthermore, each blend sample was kept at ambient temperature for about 1 month to allow crystallization to approach its equilibrium state. For blend samples prepared, the blend types and the differences in 3HP content were tabulated in Table 2.

Analytical Procedures. Molecular weights of polyester samples were measured by a Toso HLC-8020 GPC instrument with a Toso SC-8010 controller, refractive detector and TSK gel $G2000H_{XL}$ and GMH_{XL} columns. Polystyrene standards with narrow molecular weight distribution were used to construct a calibration curve, and then the number-average and weight-average molecular weights (M_n, M_w) and polydispersity (M_w/M_n) were calculated through a SC-8010 data processor. The 3HP molar fractions of the P(3HB-*co*-3HP) samples were determined from the ^1H NMR spectra measured on a JEOL GSX-270 spectrometer at 25 °C in $CDCl_3$ solution with a 4.5 μs pulse width (45° pulse), 5 s pulse repetition time, 4000 Hz spectral width, 16 K data points, and 32 FID accumulation. Thermal analyses were conducted on a Seiko DSC200U controlled through a Seiko EXSTAR6000 workstation. The samples of about 4 mg were encapsulated in aluminum pans. First, the samples were melted at 195 °C and then cooled to 30 °C and isothermally crystallized for about 1 month to erase their thermal histories. The melting temperature (T_m) and enthalpy of fusion were estimated from the DSC thermal traces measured by heating the samples from −80 to +195 °C at a rate of 10 °C min^{-1} (first scan). After rapid quenching, the glass transition temperatures (T_g) were mea-

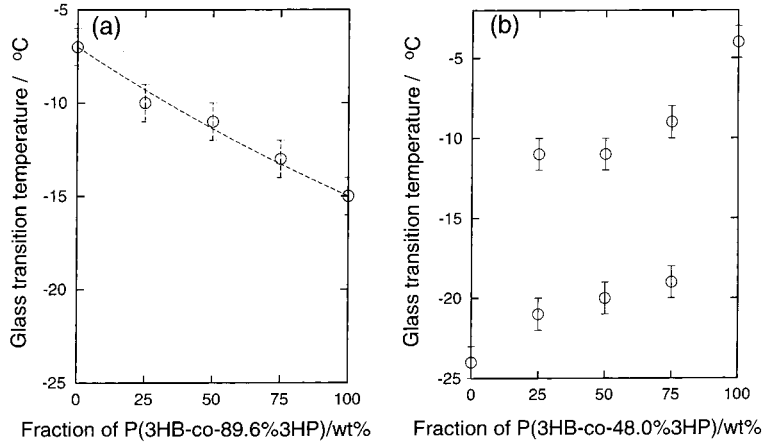

Figure 1. Blend composition dependence of glass transition temperature for blends of (a) P(3HB-*co*-60.1%3HP)/P(3HB-*co*-89.6%3HP) and (b) P(3HP)/P(3HB-*co*-48.0%3HP). The dashed line in part a indicates the results calculated by the Wood equation.

Table 3. Amorphous Phase Behavior of Blends

sample code	difference in 3HP content, %	glass transition temp(°C) 100/0	75/25	50/50	25/75	0/100
P(3HB-*co*-15.9%3HP)/P(3HB-*co*-23.8%3HP)	7.9	4	3	3	2	1
P(3HB-*co*-60.1%3HP)/P(3HB-*co*-68.7%3HP)	8.6	−7	−7	−8	−9	−10
P(3HB)/P(3HB-*co*-11.3%3HP)	11.3	6	5	5	4	3
P(3HB-*co*-48.0%3HP)/P(3HB-*co*-60.1%3HP)	12.1	−4	−5	−5	−6	−7
P(3HP)/P(3HB-*co*-86.2%3HP)	14.8	−24	−22	−21	−18	−15
P(3HB)/P(3HB-*co*-14.9%)	14.9	6	5	4	4	3
P(3HB)/P(3HB-*co*-23.8%)	23.8	6	5	3	2	1
P(3HB-*co*-68.7%3HP)/P(3HB-*co*-95.9%3HP)	27.2	−10	−11	−13	−16	−18
P(3HB-*co*-60.1%3HP)/P(3HB-*co*-89.6%3HP)	29.5	−7	−10	−11	−13	−15
P(3HP)/P(3HB-*co*-68.7%3HP)	31.3	−24	−17	−16	−12	−10
P(3HB-*co*-14.9%3HP)/P(3HB-*co*-53.1%3HP)	38.2	3	3, −6	3, −6	3, −6	−6
P(3HB)/P(3HB-*co*-39.0%3HP)	39.0	6	6, −1	6, −2	6, −2	−2
P(3HP)/P(3HB-*co*-60.1%3HP)	39.9	−24	−19, −12	−18, −12	−16, −10	−7
P(3HP)/P(3HB-*co*-48.0%3HP)	52.0	−24	−21, −11	−21, −11	−19, −9	−4
P(3HB-*co*-15.9%3HP)/P(3HB-*co*-77.9%3HP)	62.0	4	4, −11	3, −12	3, −12	−12
P(3HB)/P(3HB-*co*-77.9%3HP)	77.9	6	6, −13	6, −12	6, −12	−12
P(3HP)/P(3HB-*co*-11.3%3HP)	88.7	−24	−20, −1	−20, 2	−20, 2	3

sured by reheating the samples from −100 to +195 °C at a rate of 20 °C min^{-1} (second scan). The T_g value was estimated as the midpoint of heat capacity change in the thermal diagram by the second heating scan. The isothermal spherulitic growth rate (G) was measured on an Olympus BX90 polarizing optical microscope equipped with a Mettler FP80HT hot stage. Films of samples were first heated to 195° C and kept for 2 min and then quickly cooled to the desired isothermal crystallization temperature (T_c). The dimensions of spherulites were monitored through a Sony CCD video camera attached to the microscope. The G values were estimated from the slope, dR/dt, in which R was the radius of spherulites at a given time t.

Results and Discussion

Amorphous Phase Behavior of Blends. The miscibility was investigated in the melt for 17 kinds of blend samples prepared. Figure 1 shows the typical two types for dependence of glass transition temperature (T_g) on the weight fraction (wt %) among the data listed in Table 3. As far as the T_g of Figure 1a is concerned, it emerged from DSC analysis that the blends are characterized by a single T_g intermediate between two T_g values of the components. Moreover, T_g values, which are in good agreement with that calculated from the Wood equation,[32] are composition dependent

$$T_g = \frac{W_1 T_{g1} + K W_2 T_{g2}}{W_1 + K W_2} \quad (1)$$

with a K value of 0.8, where W_1 and W_2 are the weight fractions, T_{g1} and T_{g2} are the glass transition temperatures of the component polymers of the blend, and T_g is the glass transition temperature of the blend. The fitting variation was less than ±0.1 of the K value. Equation 1, as shown by Figure 1a, fits the experimental T_g data well, strongly suggesting that the blend systems of this type are miscible in the melt and in the amorphous state over the whole composition range. Examining of the T_g values as in Figure 1b, two glass transition temperatures between those of two components are observed on the whole range of blend composition. Hence, DSC results show melt-immiscibility of these two constituents. Table 3 summarizes the results of the glass transition temperature. These are divided into two types by the presence of one or two T_g values, which were measured by the second DSC heating scans. Table 3 shows that some blends, in which the difference in 3HP unit content between two constituent polymers is less than ca. 32 mol %, have T_g with the blend composition-dependent change. In contrast to these, those with 3HP content difference over ca. 38 mol % have two T_g values independent of blend composition. It indicates that the former cases are miscible and the latter immiscible. Therefore, it is concluded that the miscibility of P(3HB-*co*-3HP) blends depends on the differences of 3HP content between component polymers of the blends and the boundary between miscibility and immiscibility for P(3HP-*co*-3HB) components, exists in the 3HP content difference of ranges about 30−40%.

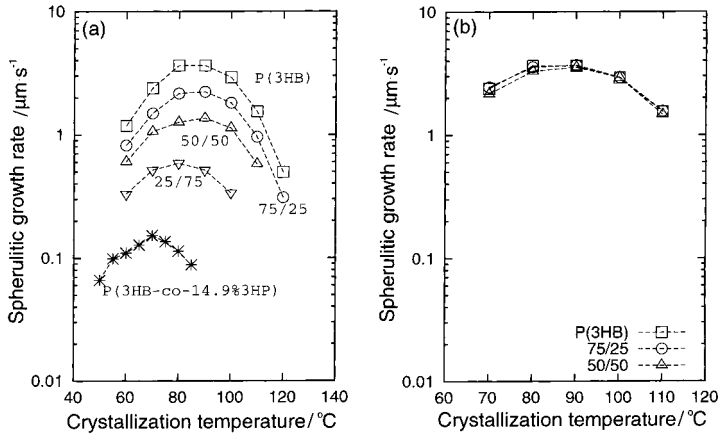

Figure 2. Spherulite growth rates of (a) P(3HB)/P(3HB-*co*-14.9%3HP) and (b) P(3HB)/P(3HB-*co*-77.9%3HP)blend systems. The P(3HB)/P(3HB-*co*-3HP) blend ratios are shown in the figures. The maximum deviation at each point is approximately ±5% of the mean values of the reading.

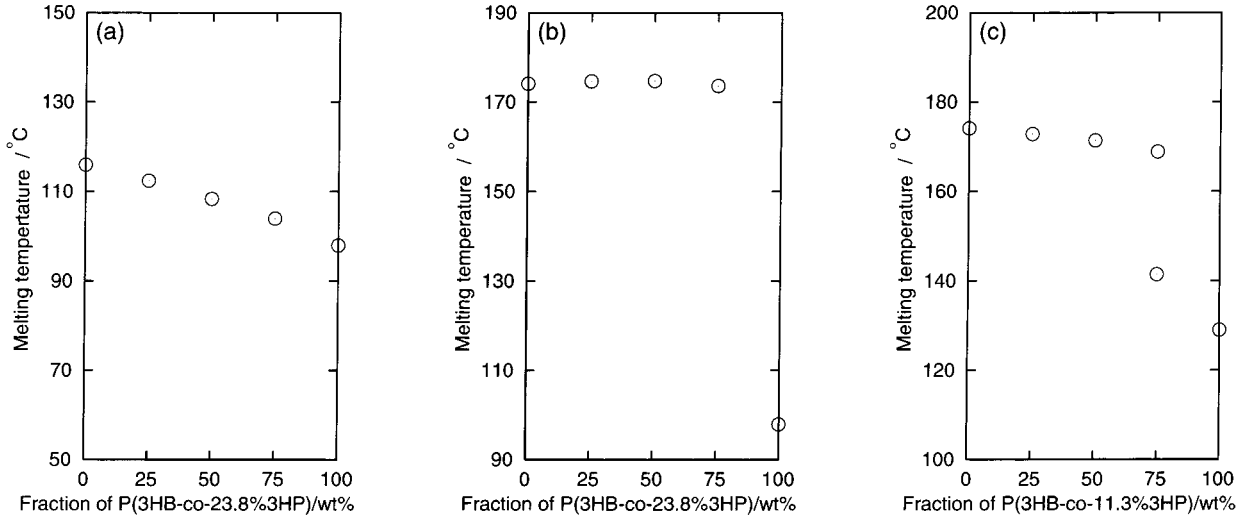

Figure 3. Blend composition dependence of melting temperatures for blends of (a) P(3HB-*co*-15.9%3HP)/P(3HB-*co*-23.8%3HP), (b) P(3HB)/P(3HB-*co*-23.8%3HP), and (c) P(3HB)/P(3HB-*co*-11.3%3HP).

Figure 2 depicts typical examples of the variability of spherulite growth rate presented as either the pure state or a component of the binary blend at various isothermal crystallization temperatures for PHB/P(3HB-*co*-14.9%3HP) and PHB/P(3HB-*co*-77.9%3HP). Each curve has the fastest growth rate in a temperature range of 70−90 °C, and the rate decreases with the change of temperature. In Figure 2a, the spherulite growth rate of the blend decreases with increase of the fraction of P(3HB-*co*-14.9%3HP) and becomes closer to that of P(3HB-*co*-14.9%3HP) for all crystallization temperatures. It is difficult to decide whether these crystals are made from only P(3HB) component or both P(3HB) and P(3HB-*co*-14.9%3HP) components. It is indicated that the crystals grow from a single amorphous phase, in which two component polymers coexisting in the blends have some interactions between themselves, because the spherulite growth rate depends on the fraction of blends. Therefore, this can be offered as the indirect evidence of miscibility in these blend systems. On the other hand, Figure 2b exhibits almost the same spherulite growth rate regardless of the blend composition. The reason is thought to be that the crystals grow from phase-separated amorphous phases, so that the one component has no effect on the crystallization of the other component. Besides, P(3HB)/P(3HB-*co*-11.3%-3HP), P(3HB)/P(3HB-*co*-14.9%3HP), P(3HB)/P(3HB-*co*-23.8%3HP), and P(3HB-*co*-15.9%3HP)/P(3HB-*co*-23.8%-3HP) blend systems have tendencies similar to that as shown in Figure 2a and P(3HB)/P(3HB-*co*-77.9%3HP), P(3HB-*co*-15.9%3HP)/P(3HB-*co*-77.9%3HP), P(3HP)/P(3HB-*co*-11.3%3HP), P(3HB)/P(3HB-*co*-39.0%3HP), and P(3HB-*co*-14.9%3HP)/P(3HB-*co*-53.1%3HP) systems similar to that shown in Figure 2b.

Crystalline Phase Behavior of Blends. Crystallization and melting behavior of blends of P(3HB-*co*-3HP) copolyesters have been investigated. In Table 2, each of binary blend systems analyzed was classified as one of four typical blend types. The detailed results are described for 11 distinct samples as the examples of those four types. The results for the other samples are not shown, because they are similar to at least one of 11 samples.

(1) Binary Blends of Two P(3HB)-Lattice Type Components [HB + HB]: P(3HB-*co*-15.9%3HP)/P(3HB-*co*-23.8%3HP), P(3HB)/P(3HB-*co*-23.8%3HP), and P(3HB)/P(3HB-*co*-11.3%3HP). The P(3HB-*co*-15.9%3HP)/P(3HB-*co*-23.8%3HP) blends may have only a single crystalline phase being formed from the miscible melt. Figures 3a, 4a, and 5a show melting temperature, T_m, heat of fusion, ΔH, and spherulite growth rate, G, of these blends against the blend-composition. The G value shown is the spherulite growth rate observed at 70 °C under a polarizing optical microscope

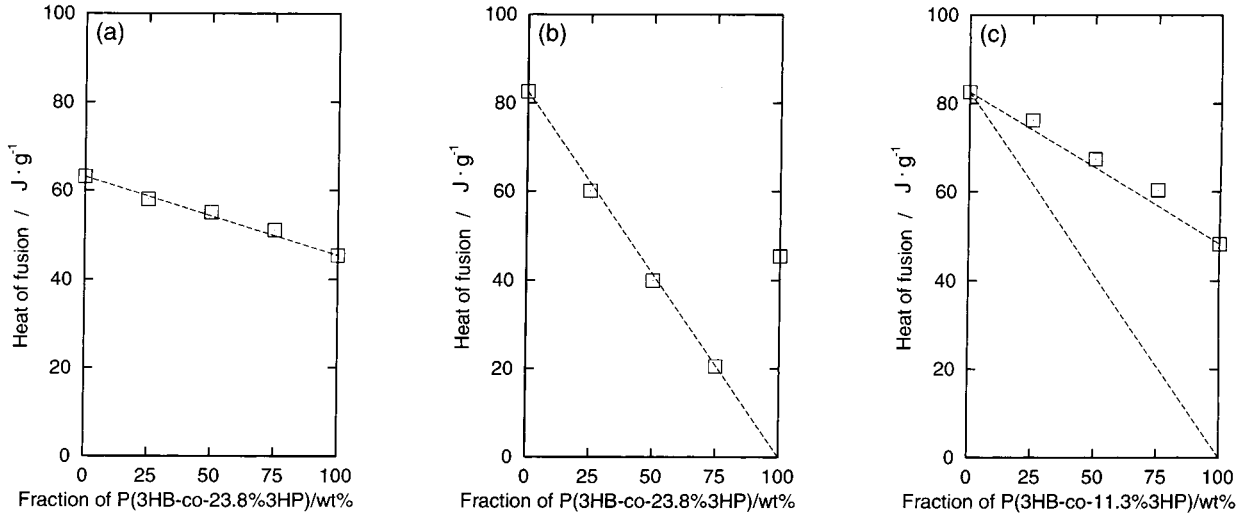

Figure 4. Blend composition dependence of heats of fusion for blends of (a) P(3HB-*co*-15.9%3HP)/P(3HB-*co*-23.8%3HP), (b) P(3HB)/P(3HB-*co*-23.8%3HP), and (c) P(3HB)/P(3HB-*co*-11.3%3HP). The dashed lines represent the values calculted by the equation $\Delta H = \Delta H_1 W_1 + \Delta H_2 W_2$ in parts a and c and $\Delta H = \Delta H_1 W_1$ ($\Delta H_2 = 0$) in part b and the extra line of part c, where W_1, W_2 are the weight fractions, ΔH_1, ΔH_2 are the heats of fusion of the component polymers of the blend, and ΔH is the heat of fusion of the blend.

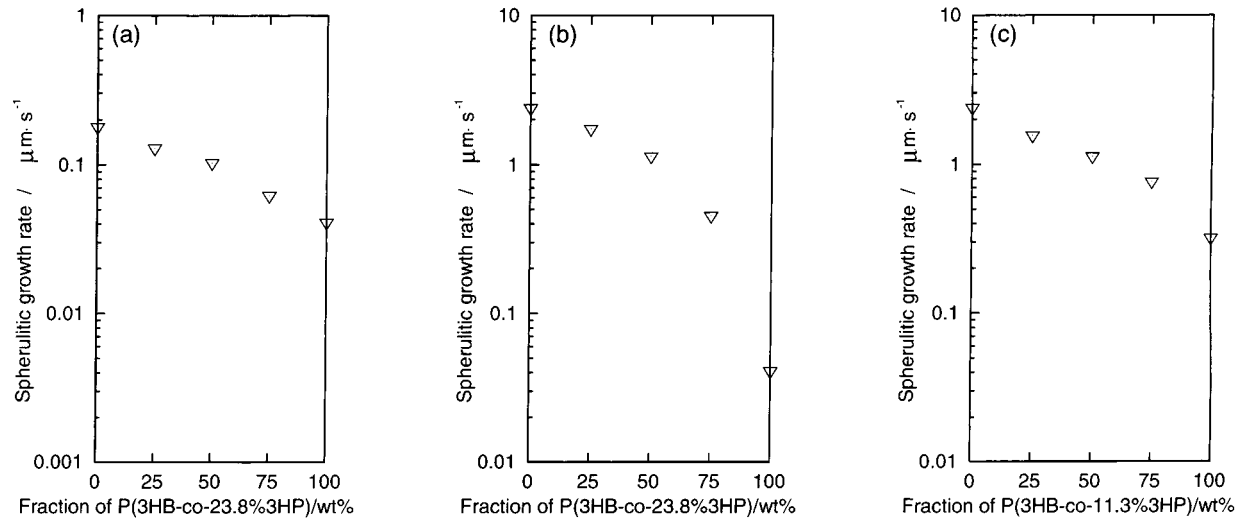

Figure 5. Blend composition dependence of spherulite growth rates for blends of (a) P(3HB-*co*-15.9%3HP)/P(3HB-*co*-23.8%3HP), (b) P(3HB)/P(3HB-*co*-23.8%3HP), and (c) P(3HB)/P(3HB-*co*-11.3%3HP) crystallized at 70 °C.

for all experiments. Although the spherulite growth rate G is not a crystallization rate of a component, it can provide some meaningful information on the crystallization. Each of the blends has single T_m, ΔH, and G which lie on an corresponding straight line connecting those of P(3HB-*co*-15.9%3HP) and P(3HB-*co*-23.8%3HP), respectively. Because the values of T_m, ΔH, and G tend to be similar to those expected for pure P(3HB-*co*-3HP) copolymers with 15.9−23.8% mol 3HP, it can be considered that the trends of blend-composition dependence of those values may represent the observation that these binary blend systems are isomorphous in the crystalline phase. Thus, the melting and crystallization behavior indicates that P(3HB-*co*-15.9%3HP)/P(3HB-*co*-23.8%-3HP) form a miscible melt followed by cocrystallization.

Figures 3b, 4b, and 5b shows T_m, ΔH, and G of P(3HB)/P(3HB-*co*-23.8%3HP) blends. These blends show a single T_m very close to that of P(3HB) and ΔH of blend is located on the straight line connecting the ΔH values of P(3HB) and $\Delta H = 0$, indicating the crystallization of only a P(3HB) component. The melting peak indicating the crystallization of P(3HB-*co*-23.8%3HP) was not observed. In Figure 5b, the depression of the G value of P(3HB) and the absence of P(3HB-*co*-23.8%3HP) spherulites suggest the presence of intermolecular interaction between P(3HB) and P(3HB-*co*-23.8%3HP). So it can be concluded that parts of P(3HB) molecules are partitioned from the miscible melt to form the crystalline phase, and during the growth of P(3HB) crystals, the P(3HB-*co*-23.8%3HP) molecules are ejected to the amorphous region, forming a homogeneous solution with uncrystallized P(3HB) molecules. Since the difference of the G value between P(3HB) and P(3HB-*co*-23.8%3HP) is so large, only P(3HB) lamella may be able to grow in the initial state crystallization, but P(3HB-*co*-23.8%3HP) molecules may be trapped in the interlamellar regions.

For P(3HB)/P(3HB-*co*-11.3%3HP) blends, the T_m s are plotted against blend composition in Figure 3c. The blends containing less than 50 wt % copolyester show a single T_m, while the blend containing 75 wt % has two T_m values. The T_m of the former blends and the higher T_m of the blend containing 75 wt % copolyester are close to that of P(3HB) in the pure state. The lower T_m of the blend containing 75 wt % copolyester and that of P(3HB-*co*-11.3%3HP) can be considered to lie on the straight

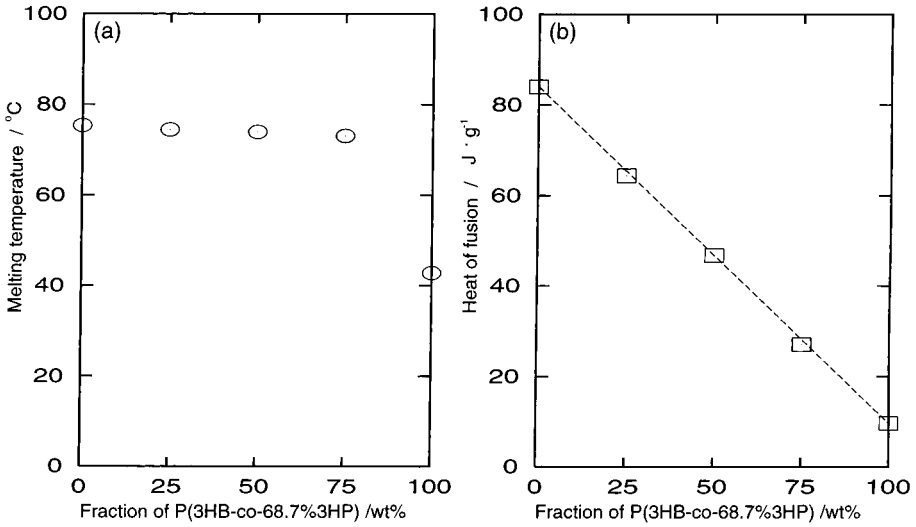

Figure 6. Blend composition dependence of (a) melting temperatures and (b) heats of fusion for blends of P(3HP)/P(3HB-*co*-68.7%3HP). The dashed line in part b are calculated by the equation used in Figure 4, parts a and c.

line connecting between the T_m values of P(3HB) and P(3HB-*co*-11.3%3HP). The ΔH and G values are shown in Figures 4c and 5c. With increase of P(3HB-*co*-11.3%3HP) fraction, the ΔH value decreases linearly along the line connecting the ΔH's of P(3HB) and P(3HB-*co*-11.3%3HP). If only the P(3HB) component is crystallized, each of the blends will have the ΔH value on the lower straight line which connects the ΔH value of pure P(3HB) and $\Delta H = 0$ as shown in Figure 4c. The changes in the G values look like those of P(3HB-*co*-15.9%3HP)/P(3HB-*co*-23.8%3HP) blends. Therefore, these blend systems show a crystallization behavior combining that of P(3HB-*co*-15.9%3HP)/P(3HB-*co*-23.8%3HP) and P(3HB)/P(3HB-*co*-23.8%3HP). In other words, these blend systems are composed of two crystalline phases; the isomorphous crystalline phase and the crystalline phase of the component polyester having the largest G value being partitioned from the miscible blend melt. As an another possibility, it should not be neglected that both of the crystalline phases made from the respective P(3HB) and P(3HB-*co*-11.3%3HP) crystalline phases may exist, for the difference of G between P(3HB) and P(3HB-*co*-11.3%3HP) is large and ΔH of P(3HB-*co*-11.3%3HP) contributes to that of each blend.

(2) Binary Blends of Two P(3HP)-Lattice Type Components [HP + HP]: P(3HP)/P(3HB-*co*-68.7%-3HP), P(3HP)/P(3HB-*co*-86.2%3HP), and P(3HB-*co*-95.9%3HP)/P(3HB-*co*-68.7%3HP). Figure 6 shows typical examples for T_m and ΔH of the blends, which are composed of P(3HP) and P(3HB-*co*-3HP) with high 3HP fraction or two P(3HB-*co*-3HP) components with high 3HP fraction as in the case of P(3HP)/P(3HB-*co*-68.7%3HP). The phase features of these blend systems are likely to be similar to those of P(3HB)/P(3HB-*co*-23.8%3HP) blends which have a single crystalline phase of the component with the larger crystallization rate. These blends of two P(3HP) lattice type components show a single T_m which is almost the same as those of P(3HP) and P(3HB-*co*-95.9%3HP). Each of the blends has a ΔH value which lies on a straight line connecting the two components. These results suggest that the P(3HP) and P(3HB-*co*-95.9%3HP) crystallize in a unique fashion, but the crystallization of the other secondary component is suppressed though it participates in the crystallization of the main component of the blends to some extent.

We cannot determine the G values of these blends using the optical microscopy at 70 °C, for that is too near to their T_ms. Cao and co-workers[16] reported that the spherulitic growth of P(3HP) in the pure or P(3HB)/P(3HP) blending state could not be precisely estimated due to the rapid nucleation, resulting in quick impingement of spherulites even at a supercooling ($T_m - T_c$) of 7−10 °C. They also showed that the average dimension of P(3HP) spherulites after impingement was about 20 μm, which is 2 orders of magnitude smaller than that of P(3HB) spherulites and is too small to follow the growth by optical microscopy. They also reported that bacterial copolyester P(3HB-*co*-95.9 mol %3HP) formed microcrystals similar to that of the chemosynthetic homopolymer P(3HP).[22] These results suggest that the spherulitic growth of P(3HP) or P(3HB-*co*-3HP) with a high fraction of 3HP monomer units occurs more rapidly than that of P(3HB) or P(3HB-*co*-3HP) with high 3HB monomer units. That is, the P(3HB-*co*-3HP) component having a lower crystallization rate is more difficult to crystallize in the blend system of two P(3HP)-lattice type components than in that of two P(3HB)-lattice type components, and it may be trapped in the interlamellar region with very small crystals, because only the crystal of the component with quicker crystallization may grow in the initial state. Therefore, in these blends, the isomorphism or the crystallization of both components seems to be more difficult, which can be pronounced in the blend system of two P(3HB)-lattice type components as above-described. Similarly, the compositional partition followed by the crystallization of one component takes place in some P(3HB)/P(3HB-*co*-3HV) blends, as reported by Yoshie and co-workers.[25]

(3) Binary Blends of P(3HB)- and P(3HP)-Lattice Type Components [HB + HP]: P(3HB)/P(3HB-*co*-77.9%3HP), P(3HP)/P(3HB-*co*-11.3%3HP), and P-(3HB-*co*-15.9%3HP)/P(3HB-*co*-77.9%3HP). As mentioned before, the blends of this type seem to be immiscible in the melt and in the amorphous region. So these blends are likely to be two crystalline phases similar to those in the pure component being formed from the immiscible melt.

Figure 7 shows the thermal behavior typical for the immiscible blends as the case of P(3HP)/P(3HB-*co*-11.3%3HP). All the blends were characterized by T_m's which are very close to those observed for the respective

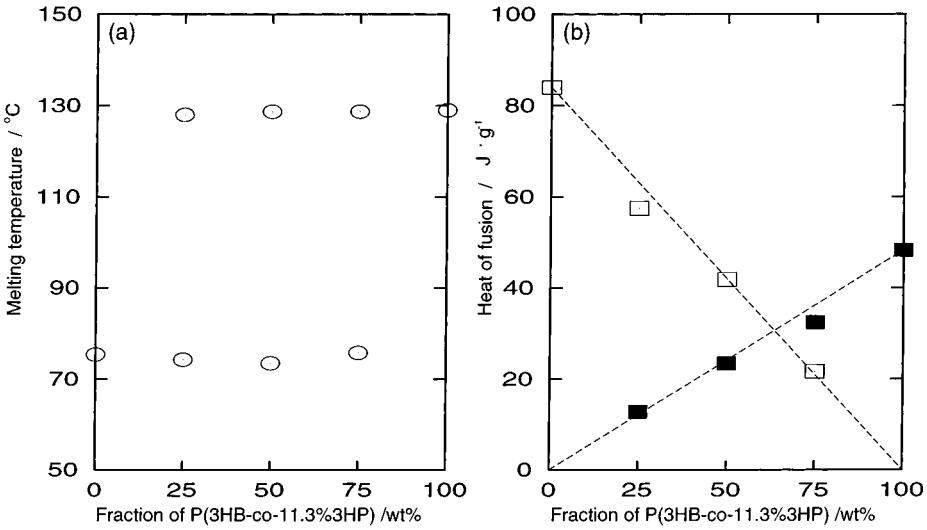

Figure 7. Blend composition dependence of (a) melting temperatures and (b) heats of fusion for blends of P(3HP)/P(3HB-*co*-11.3%3HP). The open square and filled square symbols are the heats of fusion of P(3HP) and P(3HB-*co*-11.3%3HP) portions for blends, respectively. Each dashed line is calculated from the heat of fusion for pure polymer component by the equation used in Figure 4b.

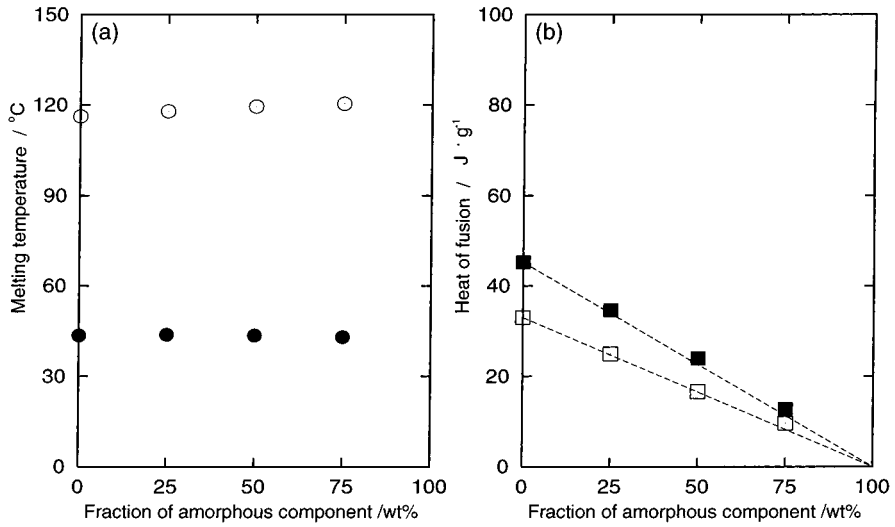

Figure 8. Blend composition dependence of (a) melting temperatures and (b) heats of fusion for blends of a crystalline and amorphous components. The open symbols are used for P(3HB-*co*-14.9%3HP)/P(3HB-*co*-53.1%3HP) and the filled symbols for P(3HB-*co*-89.6%3HP)/P(3HB-*co*-60.1%3HP). P(3HB-*co*-53.1%3HP) and P(3HB-*co*-60.1%3HP) are amorphous portions. The dashed lines of part b are calculated by the equation used in Figure 4b.

pure components. The ΔH values depend on the fraction of each component only and are independent of the blend partner. (For P(3HB-*co*-15.9%3HP)/P(3HB-*co*-77.9%3HP), the range of the endotherm peaks for the two polyesters overlap but two individual peaks are observed.) Components exert little influence on the melting behavior of the other components in a blend. Considering the behaviors of T_g mentioned before, these results provide indirect evidence for the phase separation in the melt and the crystalline phases. Polarized micrography also showed the occurrence of the phase separation. One of the melt phases formed spherulites and the other formed islands of the melt in the intraspherulite regions at the initial stage. The G values are 2.39, 2.45, 2.16 μm s^{-1} in the 100/0, 75/25, 50/50 P(3HB)/P(3HB-*co*-77.9%3HP) blends, which are very similar to that of P(3HB). Those of P(3HP)/P(3HB-*co*-11.3%3HP) and P(3HB-*co*-15.9%3HP)/P(3HB-*co*-77.9%3HP) blends are almost constant in the ranges 0.179−0.138 and 0.299−0.319 μm s^{-1} respectively, regardless of the change of blend composition. These results also indicate a phase separation.

(4) Binary Blends of the P(3HB)- or P(3HP)-Type Crystalline Component and Amorphous Component [HB or HP + AM]: P(3HB-*co*-14.9%3HP)/P(3HB-*co*-53.1%3HP) and P(3HB-*co*-89.6%3HP)/P(3HB-*co*-60.1%3HP). Figure 8 depicts the values of T_m and ΔH of the blends of crystalline/amorphous combination, namely, P(3HB-*co*-14.9%3HP)/P(3HB-*co*-53.1%3HP) and P(3HB-*co*-89.6%3HP)/P(3HB-*co*-60.1%-3HP) systems. As shown in Table 3, the former blends are immiscible and the latter miscible in the melt. The thermal behavior of these two-blend systems seem to be of the same character. The T_m values are close to those of the crystalline component, and the ΔH values also depend on the crystalline part, irrespective of the amorphous part.

Although the two blend systems are similar in that the results of T_m and ΔH depend on the only crystalline component, indifferent to the amorphous component, the origins of these for the two blends are very different. In the case of P(3HB-*co*-14.9%3HP)/P(3HB-*co*-53.1%3HP) blends, the crystalline phase was formed from the phase-separated melt. Thus, the G values are almost

the same as 0.152, 0.150, 0.158 μm s^{-1} with compositional changes 100/0, 75/25, and 50/50 (for the 25/75 blend, spherulite was not detected). On the other hand, in the case of P(3HB-*co*-89.6%3HP)/P(3HB-*co*-60.1%3HP) blends, the depression of the *G* value is expected with the increase of the content of P(3HB-*co*-60.1%3HP) component, owing to the interaction between two components, similar to Figure 5b. These spherulites are formed from one portion which can be crystallized in the same melt domain. These crystallizations resulted from a crystallization of the part which is able to crystallize from the same melt domain. These blends are similar to miscible crystalline/amorphous blend[33−35] and crystalline/crystalline blends in which one component is restrained as the melt phase.[36−39] As one of examples of the latter case, the miscible blends of P(3HB)/poly(ethylene oxide) [PEO] have been reported. In these blends, crystallization of PEO was prevented by keeping the crystallization temperature, T_c (90−140 °C), higher than T_m (ca. 60 °C) of PEO.[36] Due to miscibility between P(3HB) and PEO, the blends exhibit a single glass transition temperature, a depression of the equilibrium melting temperature of P(3HB) and a decrease of *G* in a certain T_c range (90−140 °C) with an increase of the PEO content.

Conclusion

Phase behavior and thermal properties were investigated for binary blends of compositionally well-fractionated P(3HB-*co*-3HP) samples. In the amorphous phase, the miscibility depends mainly on the difference of 3HP content (or 3HB content) between two component polymers. The boundary of 3HP content difference for miscibility is about 30−40%. For the crystalline phase, the blend samples of the following four types were examined by analyses of the DSC melting thermograms and spherulite growth rates. The type of crystal lattice, miscibility, and the difference of *G* value between two components seem to be important factors controlling the crystalline phase behavior.

It is worth comparing these results of the blends of compositionally well-fractionated polymers, with those of unfractionated bacterial P(3HB-*co*-3HP) copolymers. In a previous paper,[31] unfractionated bacterial P(3HB-*co*-19.4%3HP) samples can be regarded as a ternary blend of 1/2/4 P(3HB-*co*-25.0%3HP)/P(3HB-*co*-11.3%3HP)/P(3HB-*co*-14.9%3HP). The differences in the 3HP content between two of these three components are 13.7%, 3.6%, and 10.1%. According to the results found in this article,[31] unfractonated P(3HB-*co*-19.4%3HP) sample may be classified as a blend system in which component polymers are miscible in the amorphous state and those having larger crystallization rate preferentially (co)-crystallize. This prediction is consistent with the observation that this unfractionated P(3HB-*co*-19.4%3HP) sample shows distinct melting peaks corresponding to those of pure P(3HB-*co*-25.0%3HP), P(3HB-*co*-11.3%3HP), and P(3HB-*co*-14.9%3HP) components and T_g, ΔH, and *G* represent the values between those of P(3HB-*co*-11.3%3HP) and P(3HB-*co*-25.0%3HP) fractions. Therefore, the effect of the compositional distribution of P(3HB-*co*-3HP) bacterial copolymer on the physical properties should be considered in the physical characterization and also in the practical use of P(3HB-*co*-3HP) copolymers.

Acknowledgment. This work was partially supported by a Grant-in-Aid for Scientific Research on Priority Area, "Sustainable Biodegradable Plastics", No.11217205 (2000) from the Ministry of Education, Science, Sports and Culture (Japan).

References and Notes

(1) Doi, Y. *Microbial Polyester*; VCH Publisher: New York, 1990.
(2) Inoue, Y.; Yoshie, N. *Prog. Polym. Sci.* **1992**, *17*, 571.
(3) Hocking, P. J.; Marchessault, R. H. *Biodegradable Polymers*; Griffin, G. J. L., Ed.; Blackie Academic & Professional: London, New York, 1994.
(4) Holmes, P. A.; Wright, L. F.; Collins, S. H. Eur. Pat. Appl. 0 052 459, 1981; Eur. Pat. Appl. 0 069 497, 1983.
(5) Holmes, P. A. *Phys. Technol.* **1995**, *16*, 32.
(6) Doi, Y.; Tamaki, A.; Kunioka, M.; Soga, K. *Appl. Microbiol. Biotechnol.* **1988**, *28*, 330.
(7) Nakamura, S.; Kunioka, M.; Doi, Y. *Macromol. Rep.* **1991**, *A28* (Suppl. 1), 15.
(8) Hiramatsu, M.; Doi, Y. *Polymer* **1993**, *34*, 4782.
(9) Shimamura, E.; Scandola, M.; Doi. Y. *Macromolecules* **1994**, *27*, 4429.
(10) Ichikawa, M.; Nakamura, K.; Yoshie, N.; Asakawa, N.; Inoue, Y. *Macromol. Chem. Phys.* **1996**, *197*, 2467.
(11) Cao, A.; Ichikawa, M.; kasuya, K.; Yoshie, N.; Asakawa, N.; Inoue, Y.; Doi. Y.; Abe, H. *Polym. J.* **1996**, *28*, 1096.
(12) Nakamura, K.; Yoshie, N.; Sakurai. M.; Inoue, Y. *Polymer* **1994**, *35*, 193.
(13) Spyros, A.; Marchessault, R. H. *Macromolecules* **1995**, *28*, 6108.
(14) Shi, F.; Ashby, R. D.; Gross, R. A. *Macromolecules* **1997**, *30*, 2521.
(15) Cao, A.; Ichikawa, M.; Ikejima, T.; Yoshie, N.; Inoue, Y. *Macromol. Chem. Phys.* **1997**, *198*, 3539.
(16) Cao, A.; Kasuya, K.; Abe, H.; Doi, Y.; Inoue, Y. *Polym. J.* **1998**, *30*, 743.
(17) Yoshie, N.; Inoue, Y. *Int. J. Biol. Macromol.* **1999**, *25*, 193.
(18) Yoshie, N.; Menju, H.; Sato, H.; Inoue, Y. *Macromolecules* **1995**, *28*, 6516.
(19) Kamiya, N.; Yamamoto, Y.; Inoue, Y.; Chujo, R.; Doi, Y. *Macromolecules* **1989**, *22*, 1676.
(20) Mitomo, H.; Morishita, N.; Doi, Y. *Polymer* **1995**, *36*, 2573.
(21) Mitomo, H.; Morishita, N.; Doi, Y. *Macromolecules* **1993**, *26*, 5809.
(22) Cao, A.; Kasuya, K.; Abe, H.; Doi, Y.; Inoue, Y. *Polymer* **1998**, *39*, 4801.
(23) Hildebrand, J.; Scott, R. *Solubility of nonelectrolytes*, 2nd ed.; Reinhold: New York, 1949.
(24) Burrell, H. *Off. Dig. Fed. Soc. Paint Technol.* **1955**, *27*, 726.
(25) Yoshie, N.; Menju, H.; Sato, H.; Inoue, Y. *Polym. J.* **1996**, *28*, 45.
(26) Barham, P. J.; Organ, S. J. *J. Mater. Sci.* **1994**, *29*, 1676.
(27) Organ, S. J.; Barham, P. J. *Polymer* **1993**, *34*, 459.
(28) Organ, S. J. *Polymer* **1994**, *35*, 86.
(29) Cao, A.; Asakawa, N.; Yoshie, N.; Inoue, Y. *Polymer* **1999**, *40*, 3309.
(30) Cao, A.; Arai, Y.; Yoshie, N.; Kasuya, K.; Doi, Y.; Inoue, Y. *Polymer* **1999**, *40*, 6821.
(31) Arai, Y.; Cao, A.; Yoshie. N.; Inoue. Y. *Polym. Int.* **1999**, *48*, 1219.
(32) Wood, L. A. *J. Polym. Sci.* **1958**, *28*, 319.
(33) Talibuddin, S.; Wu, L.; Runt, J.; Lin, J. S. *Macromolecules* **1996**, *29*, 7527.
(34) Talibuddin, S.; Runt, J.; Liu, L. Z.; Chu, B. *Macromolecules* **1998**, *31*, 1627.
(35) Wu, L.; Lisowski, M.; Talibuddin, S.; Runt, J. *Macromolecules* **1999**, *32*, 1576.
(36) Avella, M.; Martuscelli, E. *Polymer* **1988**, *29*, 1731.
(37) Avella, M.; Martuscelli, E.; Greco. P. *Polymer* **1991**, *32*, 1647.
(38) Avella, M.; Martuscelli, E.; Ramio. M. *Polymer* **1993**, *34*, 3234.
(39) Chen, H. L.; Wang, S. F. *Polymer* **2000**, *41*, 5157.

MA010270H